1926 *Chem. Mater.* **2010,** *22,* 1926–1932
DOI:10.1021/cm9037044

CHEMISTRY OF MATERIALS
Article

Nanoarchitectured TiO_2/SnO: A Future Negative Electrode for High Power Density Li-Ion Microbatteries?

Gregorio F. Ortiz,*[,a,b] Ilie Hanzu,[a] Pedro Lavela,[b] Philippe Knauth,[a] José L. Tirado,[b] and Thierry Djenizian[a]

[a]*University of Aix-Marseille I, II, III-CNRS Laboratoire Chimie Provence* (*UMR 6264*), *Electrochemistry of Materials Research Group, Centre Saint-Jérôme, F-13397 Marseille Cedex 20, France, and* [b]*Laboratorio de Química Inorgánica, Universidad de Córdoba, Edificio Marie Curie, Campus de Rabanales, 14071 Córdoba, Spain*

Received December 9, 2009. Revised Manuscript Received January 19, 2010

The synthesis of a nanoarchitectured composite material consisting of tin and tin oxide nanowires grown onto titania nanotubes by anodization of titanium and tin electrodeposition is reported. The crystallinity of the electrodes can be tuned by optional heat treatment, but the initial morphology is preserved. XRD patterns revealed the presence of Sn onto an amorphous titania matrix and Sn/SnO onto a crystalline titania matrix. Here, we highlight that tin and tin oxide nanowires are obtained when using a titania nanotubes matrix. This particular morphology is not obtained using a titania compact seed layer. Their different electrochemical behavior in lithium test cells is studied by a galvanostatic technique at a rate of 100 and 50 μA cm^{-2}. Only tin and tin oxides are checked as electroactive material by limiting voltage ranges to 1.2 and 0.01 V. The nanocomposite with this particular geometry (2 μm of tin/tin oxide thickness) has a remarkable reversible capacity of about 140 μA h cm^{-2} which is kept about 85% over 50 cycles. It is demonstrated that the matrix based on titania nanotubes can allow the volume expansion of lithium−tin alloys and thus enhances the electrochemical performances as compared with usual tin-based electrodes. The obtained capacities compare very favorably with the best literature data for Li-ion microbatteries.

Introduction

Li-ion microbatteries have emerged as a new microscale technology (MT) since in 1990 the concept of a "rocking-chair" type of rechargeable battery was introduced for first time.[1] Afterwards, Fuji photo film announced in 1997 the potential use of tin-containing oxides as promising anodes for the replacement of graphite.[2] More recently, Sony has commercialized a new battery named "Nexelion" that utilizes a tin-based amorphous anode.[3] Elemental tin and tin oxides show important advantages as compared to graphite such as higher specific capacities—especially volumetric (9090 mA h cm^{-3}), being above the newer silicon option (8322 mA h cm^{-3})—and improved safety. A major drawback of tin-based electrodes is the giant volume changes on lithium insertion/deinsertion that lead to cracks in the particles with the subsequent electronic isolation and loss of electrochemical activity. The preparation of new forms of tin-based materials with tailored particle size, morphology, and crystallinity and confinement of tin species in different matrixes define the current state of the art for reducing the above-mentioned undesirable effects. For instance, tin-based materials are prepared using sophisticated matrixes such carbonaceous substrates,[4−8] or titania,[9−11] or are fabricated in nanostructured arrangements,[12−14] forming alloys and intermetallic compounds[15−18] or coated with phosphate-based inactive matrix[9,19] among others.

*Corresponding author. E-mail: q72maorg@uco.es.

(1) Fong, R.; Sacken, U.; Dahn, J. R. *J. Electrochem. Soc.* **1990**, *137*, 2009.
(2) Idota, Y.; Kubota, T.; Matsufuji, A.; Maekawa, Y.; Miyasaka, T. *Science* **1997**, *276*, 1395.
(3) http://www.sony.net/SonyInfo/News/Press/200502/05-006E/ (last access: 9/12/2009)
(4) Grigoriants, I.; Soffer, A.; Salitra, G.; Aurbach, D. *J. Power Sources* **2005**, *146*, 185.
(5) Tirado, J. L.; Santamaria, R.; Ortiz, G. F.; Menendez, R.; Lavela, P.; Jimenez-Mateos, J. M.; Gomez Garcia, F. J.; Concheso, A.; Alcantara, R. *Carbon* **2007**, *45*, 1396.
(6) Du, N.; Zhang, H.; Chen, B.; Ma, X.; Huang, X.; Tu, J.; Yang, D. *Mater. Res. Bull.* **2009**, *44*, 211.
(7) Xu, C.; Sum, J.; Gao, L. *J. Phys. Chem. C* **2009**, *113*, 20509.
(8) Chen, J. S.; Cheah, Y. L.; Chen, Y. T.; Jayaprakash, N.; Madhavi, S.; Yang, W. H.; Lou, X. W. *J. Phys. Chem. C* **2009**, *113*, 20504.
(9) Ortiz, G. F.; Hanzu, I.; Knauth, P.; Lavela, P.; Tirado, J .L.; Djenizian, T. *Electrochem. Solid-State Lett.* **2009**, *12*, A186.
(10) Hernández, A. M.; Cerón, N. M.; Páez, J. E. R. *Rev. Fac. Ing., Univ. Antioquia* **2008**, *44*, 43.
(11) Roginskaya, Y. E.; Chibirova, F. Kh.; Kulova, T. L.; Skundin, A. M. *Russ. J. Electrochem.* **2006**, *42*, 355.
(12) Uchiyama, H.; Hosono, E.; Honma, I.; Zhou, H.; Imai, H. *Electrochem. Commun.* **2008**, *10*, 52.
(13) Zhu, L.; Yang, H.; Jin, D.; Zhu, H. *Inorg. Mater.* **2007**, *43*, 1307.
(14) Meduri, P.; Pendyala, C.; Kumar, V.; Sumanasekera, G. U.; Sunkara, M. K. *Nano Lett.* **2009**, *9*, 612.
(15) Beaulieu, L. Y.; Larcher, D.; Dunlap, R. A.; Dahn, J. R. *J. Electrochem. Soc.* **2000**, *147*, 3206.
(16) Winter, M.; Besenhard, J. O. *Electrochim. Acta* **1999**, *45*, 31.
(17) Mukaibo, H.; Osaka, T.; Reale, P.; Panero, S.; Scrosati, B.; Wachtler, M. *J. Power Sources* **2004**, *132*, 225.
(18) Hassoun, J.; Panero, S.; Scrosati, B. *J. Power Sources* **2006**, *160*, 1336.
(19) Kim, T. J.; Son, D.; Cho, J.; Park, B.; Yang, H. *Electrochim. Acta* **2004**, *49*, 4405.

Published on Web 02/01/2010

In this work we propose novel routes for preparing alternative anodes with a desired geometry to relate innovating points for the fabrication of commercial Sn-based electrodes for Li-ion batteries and microbatteries. However, the present work can find applications in different fields including chemical sensor arrays[20,21] and nanoscaled electronic devices such as nano-FETs (field effect transistors) and LEDs (light emitting diodes).[22,23] These results may provide some tricky points to reach a desired geometry path to develop innovative strategies for fabrication for commercial products in these areas.

The basic knowledge of this approach is the validity of a simple procedure to fabricate Sn and Sn/SnO nanowires (nw-Sn, nw-SnO) supported on an array of electrochemically active titania nanotubes ($ntTiO_2$) as has been demonstrated in our previous work.[24−27] The initial formation of Li_xntTiO_2 will provide an electrically conductive and ionically permeable matrix, chemically compatible with SnO.[9,11,28,29] Moreover, the nanowire structure of the tin-based materials can be beneficial for avoiding electrode cracking due to the large volume changes on cycling the electrodes. We will show that the combination of this morphology allows efficient 1D electron transport and facile strain relaxation of the electroactive material cycled between 1.2 and 0.01 V in lithium cells.

Experimental Section

In this work titanium foils from Aldrich, with a thickness of 0.127 mm and 99.7% purity, were cut and cleaned using similar procedure as in refs 28 and 29. The electrochemical anodization consisted of applying a constant voltage of 20 V during 240 min and was performed using the following cell: (i) the working electrode was a piece of Ti (0.3848 cm^2), (ii) the counter electrode was a platinum grid (1.5 cm^2), and (iii) the electrolyte was 50 mL of 1 M H_3PO_4 + 1 M NaOH + 0.5 wt % HF solution. The homemade cell used allowed the anodization of only one side of the Ti foil. We are showing results (morphological characterization and electrochemical reaction vs Li) of nanotubes and nanowire-like electrodes using the latter cell configuration. The compact layer TiO_2 was prepared by using a similar procedure in which HF was not added. In the next step, tin electrodeposition was carried out in an electrolytic bath containing Sn^{2+} ions as electroactive species. The bath consisted of tin chloride ($SnCl_2$, Sigma-Aldrich, 98%) and sodium citrate ($Na_3C_6H_5O_7 \cdot 2H_2O$, Aldrich, 99%) with a molar ratio of 0.32 at pH = 6. The citrate is used to stabilize Sn^{2+} species in solution and avoid the precipitation of tin hydroxide. We employed a three-electrode cell, in which the working electrode was the $ntTiO_2$ layer and/or the compact oxide layer ($CL\text{-}TiO_2$), the reference electrode was a commercial saturated calomel electrode (SCE), and a platinum grid acted as counter electrode. The electrodeposition experiments were carried out galvanostatically at room temperature with a current density of 1 mA cm^{-2} during 3 min. Considering Faraday's law the estimated mass for tin electrodeposited is 0.22 mg per squared centimeter of titania nanotubes. Both anodization and electrodeposition experiments were carried out using an EG&G PARSTAT 2273 potentiostat/galvanostat. Besides the as-prepared sample, additional annealed samples were prepared by a thermal treatment in air at 350 °C during 3 h with a heating/cooling rate of 60 °C/h for both $nt\text{-}TiO_2$ and $CL\text{-}TiO_2$ seed layer.

A Siemens D5000 diffractometer with Cu Kα radiation (1.5406 Å) and graphite as the monochromator was used for recording the X-ray diffraction (XRD) patterns. A 0.2° (2θ)/min velocity scan was used. The surface morphologies of the as-deposited films at room temperature and after heating were observed using scanning electron microscopy (SEM) with a Philips XL-30 FEG SEM.

The electrochemical performance of the Sn-based electrodes was studied by experiments in lithium Swagelok-type test cells. They were assembled in an argon-filled glovebox in which moisture content and oxygen level were less than 2 ppm. The electrolyte (EC; ethylcarbonate $C_3H_4O_3$, DEC: diethylcarbonate $C_5H_{10}O_3$) was embedded in a Whatman glass microfiber acting as a separator. For the discharge/charge, a constant current density of 100 and 50 μA cm^{-2} (4C and 2C respectively, here C means the total capacity of the cell obtained after 1 h) were applied to the assembled cells in the range between 1.2 and 0.01 V using an Arbin potentiostat/galvanostat multichannel system. In this work, areal capacities (μA h cm^{-2}) are given for charge and discharge because the applications of this nanocomposite Sn-based electrode would be mostly microbatteries. However, the gravimetric and volumetric capacities are expressed in the text. For these experiments no additives such as poly(vinyl difluoride), that act as binder agents, and carbon black (conductive agent) were used.

Results and Discussion

The concept of using one-dimensional (1D) nanomaterials has been demonstrated in previous work for carbon,[30] SnO_2 and Sn-based,[31,32] Si,[33,34] Co_3O_4,[35] TiO_2,[28,29,36]

(20) Harrison, P. G.; Willett, M. J. *Nature* **1988**, *332*, 337.
(21) Lee, D. S.; Shim, C. H.; Lim, J. W.; Huh, J. S.; Lee, D. D.; Kim, Y. T. *Sens. Actuators, B* **2002**, *83*, 250.
(22) Dattoli, E. N.; Wan, Q.; Guo, W.; Chen, Y. B.; Pan, X. Q.; Lu, W. *Nano Lett*. **2007**, *7*, 2463.
(23) Li, Y.; Qian, F.; Xiang, J.; Lieber, C. M. *Mater. Today* **2006**, *9*, 18.
(24) Premchand, Y. D.; Djenizian, T.; Vacandio, F.; Knauth, P. *Electrochem. Commun*. **2006**, *8*, 1840.
(25) Djenizian, T.; Hanzu, I.; Premchand, Y. D.; Vacandio, F.; Knauth, P. *Nanotechnology* **2008**, *19*, 205601.
(26) Djenizian, T.; Hanzu, I.; Eyraud, M.; Santinacci, L. *C. R. Chim*. **2008**, *11*, 995.
(27) Hanzu, I.; Djenizian, T.; Ortiz, G. F.; Knauth, P. *J. Phys. Chem. C* **2009**, *113*, 20568.
(28) Ortiz, G. F.; Hanzu, I.; Djenizian, T.; Lavela, P.; Tirado, J. L.; Knauth, P. *Chem. Mater*. **2009**, *21*, 63.
(29) Ortiz, G. F.; Hanzu, I.; Knauth, P.; Lavela, P.; Tirado, J. L.; Djenizian, T. *Electrochim. Acta* **2009**, *54*, 4262.
(30) Che, G.; Lakshmi, B. B.; Fisher, E. R.; Martin, C. R. *Nature* **1998**, *393*, 346.
(31) Park, M. S.; Wang, G. X.; Kang, Y. M.; Wexler, D.; Dou, S. X.; Liu, H. K. *Angew. Chem., Int. Ed*. **2007**, *46*, 750.
(32) Bazin, L.; Mitra, S.; Taberna, P. L.; Poizot, P.; Gressier, M.; Menu, M. J.; Bernabé, A.; Simon, P.; Tarascon, J. M. *J. Power Sources* **2009**, *188*, 578.
(33) Fleischauer, M. D.; Li, J.; Brett, M. J. *J. Electrochem. Soc*. **2009**, *156*, A33.
(34) Candace, K. C.; Hailin, P.; Gao, L.; McIlwrath, K.; Zhang, X. F.; Huggins, R. A.; Cui, Y. *Nat. Nanotechnol*. **2008**, *3*, 31.
(35) Shaju, K. M.; Jiao, F.; Debart, A.; Bruce, P. G. *Phys. Chem. Chem. Phys*. **2007**, *9*, 1837.
(36) Armstrong, G.; Armstrong, A. R.; Bruce, P. G.; Reale, P.; Scrosati, B. *Adv. Mater*. **2006**, *18*, 2597.

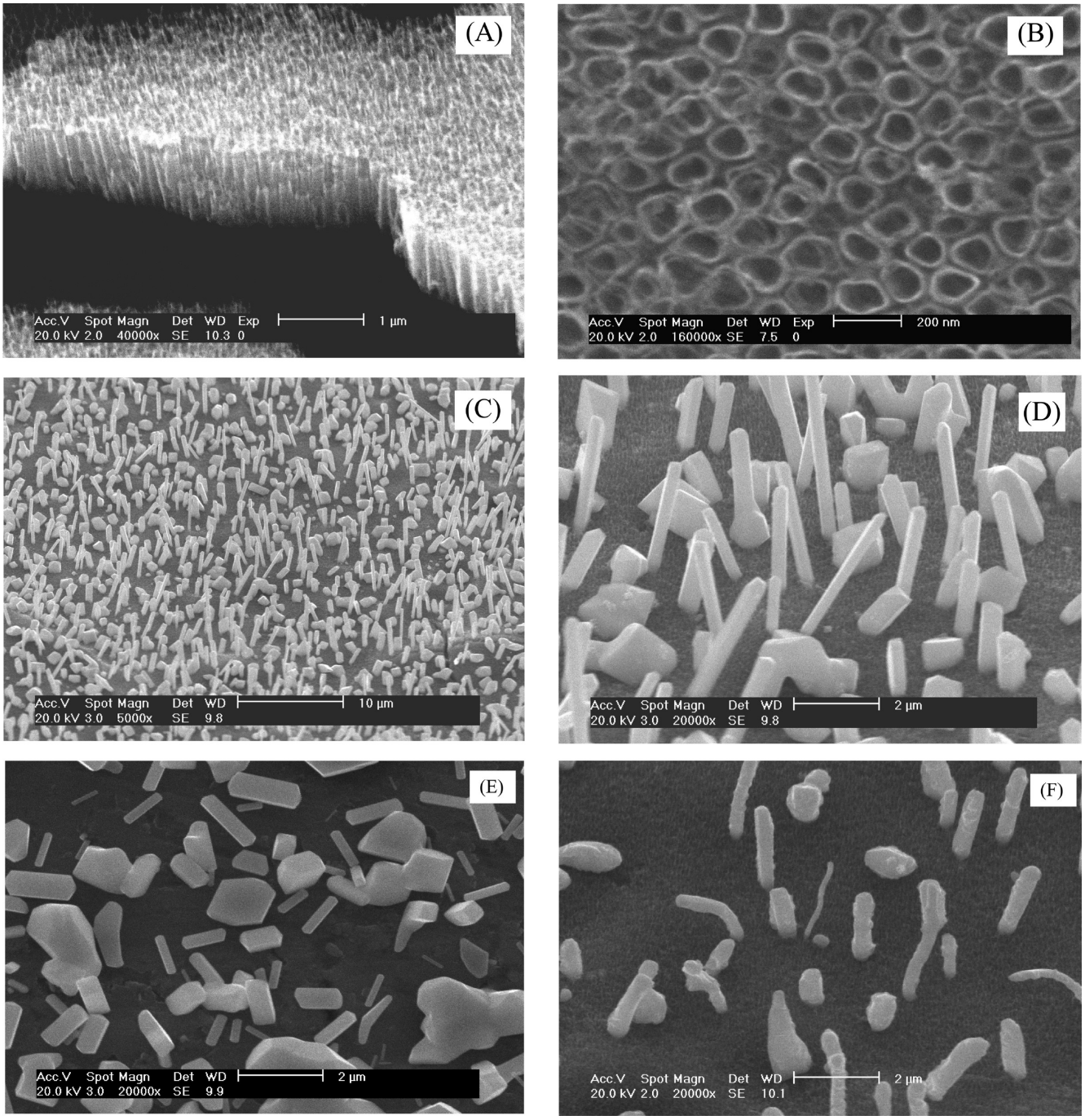

Figure 1. SEM images of (a, b) $ntTiO_2$ nanotubes from cross-section and top view image. Images taken at an angle of 40° for (c, d) tin nanowires supported onto $ntTiO_2$, (e) Sn onto TiO_2 compact layer, and (f) nwSnO onto crystalline $ntTiO_2$.

lithium nickel vanadates,[37] and V_2O_5 thin film electrodes,[38] and has shown better performances compared to bulk materials. Compared with previous studies in which micrometer sized particles were used as potential electrodes, the capacity fading and the poor lifetime observed are attributed to cracking, pulverization, and loss of electrical contact between the active material and the current collector because no free space is available for buffering the volume expansion of electrodes during lithium insertion.

Figure 1a,b shows cross-sectional and top view SEM images of as-prepared $ntTiO_2$ and tin electrochemically deposited onto $ntTiO_2$ (Figure 1c,d) and on compact layer (C.L.) TiO_2 (Figure 1e) as well as nwSnO obtained after annealing at 350 °C (Figure 1f). The parallel orientation of the nanotubes in the self-organized array yields void spaces both outside and inside the nanotubular structure. The surface of $ntTiO_2$ is covered by nwSn and nwSnO. Different morphologies are observed, with nanowires 2 μm in length and approximately 20 nm in diameter prevailing. Nucleation and growth occurs on titania nanotube layers as checked by cyclic voltammetry; the concentration of the electrodeposition bath has a great

(37) Reddy, M. V.; Wannek, C.; Pecquenard, B.; Vinatier, P.; Levasseur, A. *J. Power Sources* **2003**, *119*, 101.
(38) Gies, A.; Pecquenard, B.; Benayad, A.; Martinez, H.; Gonbeau, D.; Fuess, H.; Levasseur, A. *Thin Solid Films* **2008**, *516*, 7271.

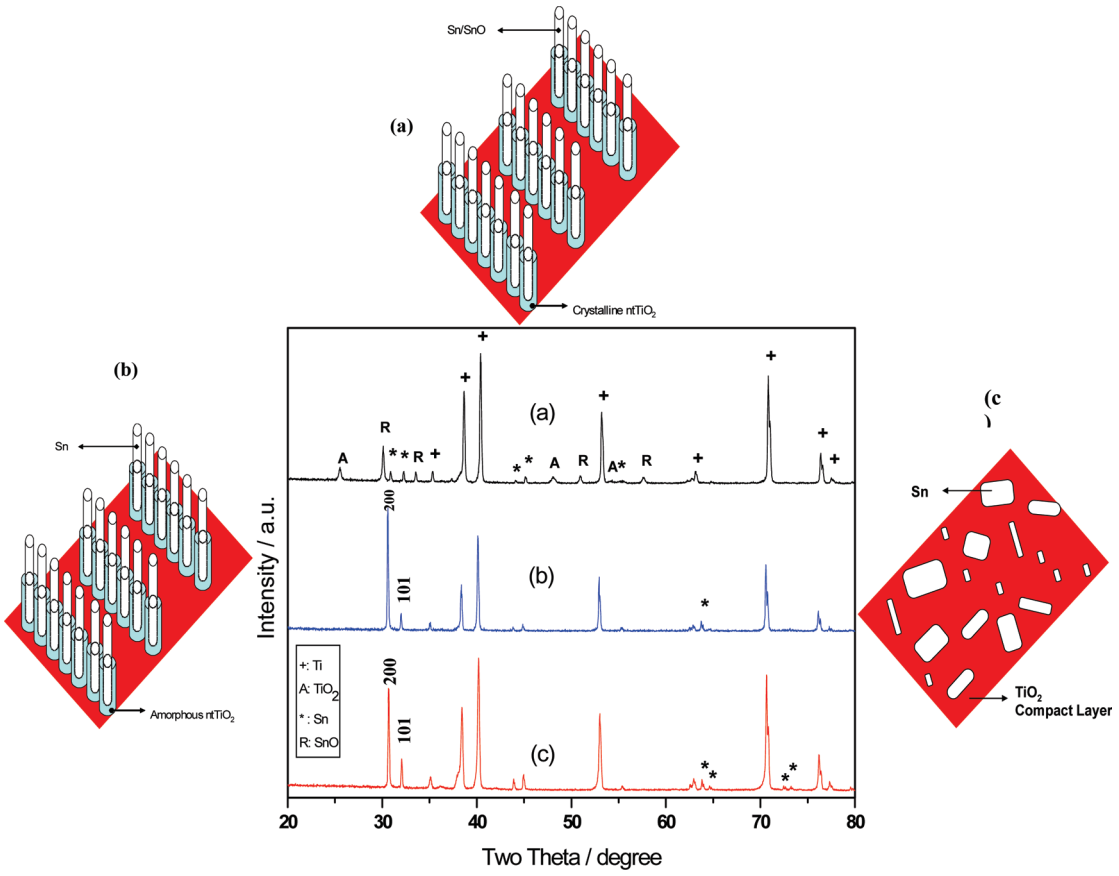

Figure 2. X-ray diffraction and schematic of the morphological outline of nanoarchitectured tin-based/$nTiO_2$ electrodes: (a) nwSn/SnO supported on $ntTiO_2$ at 350 °C, (b) nwSn onto as prepared $ntTiO_2$, and (c) Sn onto CL-TiO_2.

influence on the morphology of the deposit and the Sn wire dimensions.[27] Here tin and tin oxide nanowires exhibit an average length of about 2 μm whatever the temperature of preparation. The mechanistic study of tin electrodeposition onto TiO_2 nanotube layers and the thermodynamics, kinetics, nucleation, and growth modes are well detailed in ref 27. These parallel oriented nanostructures are likely influenced by the alignment of the $ntTiO_2$ supporting them. For the samples deposited on a CL-TiO_2, similar morphologies are observed in the tin deposited species. However, larger particle sizes are present. Nanowires with similar sizes appear horizontally laying on the flat surface evidencing the orientational effect of the $ntTiO_2$ seed layer. According to these results, the schematic representation of the different configurations of tin species nanowires deposited onto $ntTiO_2$ anode shown in Figure 2 was derived.

In Figure 2a,c are given the XRD patterns of Sn crystallites electrodeposited on annealed $ntTiO_2$, on as-prepared $ntTiO_2$, and on as-prepared C.L. TiO_2, respectively. The corresponding morphologies of Sn crystallites are also schematically depicted. When Sn is electrodeposited on as-prepared TiO_2 layers only reflections of the metal can be detected at room temperature. No peak related to the presence of tin oxide can be found in Figure 2b,c. Clearly, compared with the XRD pattern shown in Figure 2c, the preferred growth orientation of Sn crystallites grown on $ntTiO_2$ (Figure 2b) can be identified by the higher intensity ratio between the (200) and (101) diffraction. After annealing treatment, the XRD patterns show additional peaks that are attributed to the formation of SnO. Despite a strong decrease, the intensity of peaks related to the Sn metal are still detected suggesting that the oxidation of nwSn into nwSnO is not complete. In accordance with previous work, it can be noted that amorphous titania is crystallized after the thermal treatment. All these results are in agreement with previous results recently reported.[9,25,28,29]

Cycling life study is shown in Figure 3a. First reversible capacities at a rate of 100 μA cm^{-2} are very similar for three electrodes ranging between 90 and 110 μA h cm^{-2}. A remarkable characteristic in capacity retention of 70% from the initial capacity (95 μA h cm^{-2}) was obtained for crystalline the $ntTiO_2$/nw-SnO electrode, which presents higher capacities on cycling as compared with amorphous $ntTiO_2$/nw-Sn and CL-TiO_2/Sn (12% over 50 cycles). At constant current density of 50 μA cm^{-2}, they showed even better performance: initial capacity was 140 μA h cm^{-2} with an efficiency of 85% over 50 cycles. The rates for most of the tin-based bulk electrodes are low, ranging between C/10 and C/20. Here, we show that is possible to use these nanoarchitectured electrodes under 4C and 2C rates, meaning that they are very attractive for practical use in commercial batteries, which demand high power density.[7,8] Capacities presented here for a nwSnO and $ntTiO_2$ thickness of 2 and 1 μm, respectively, are really

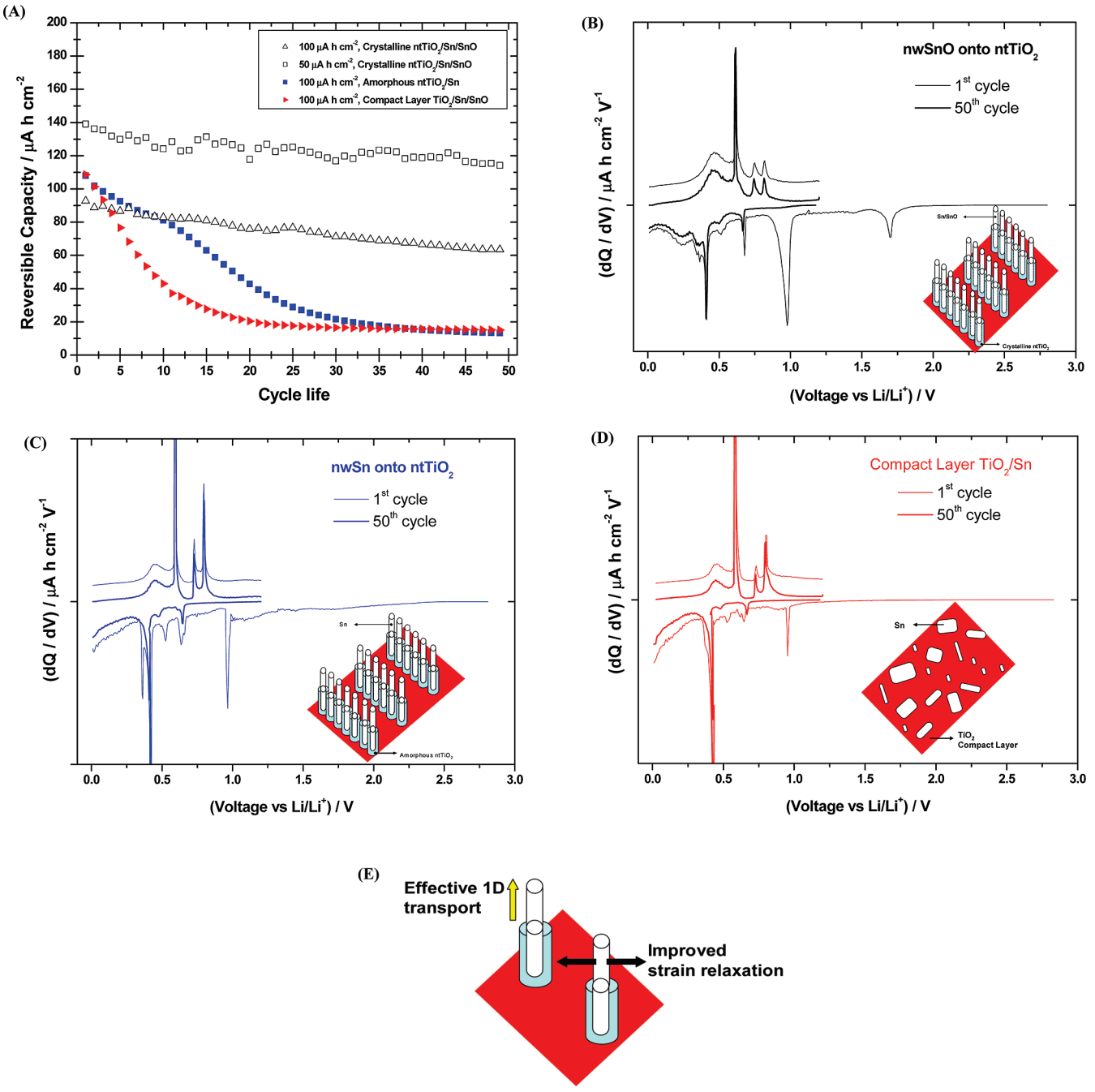

Figure 3. (a) Cycle life performance under galvanostatic regime at current density of 100 μA cm^{-2} and derivative curves for (b) crystalline nwSnO/ntTiO$_2$, (c) amorphous nwSn/ntTiO$_2$, and (d) compact layer TiO$_2$/Sn electrodes. For the crystalline sample, a current density of 50 μA cm^{-2} was used to evaluate enhanced electrochemical behavior. (e) Schematic representation of morphological changes that occur in tin-based electrodes (especially nwSnO/ntTiO$_2$) during electrochemical cycling. Here, we highlight an improved strain relaxation in the nanowires that allows them to increase in diameter and length without breaking, and the nanowires anode configuration is capable for efficient 1D electron transport.

attractive in terms of high kinetics when compared with other thin layer-based electrodes, for example, a Sn-based nanoarchitectured electrode (57 and 90 μA h cm^{-2} at C/2 rate for Sn deposited onto Cu pillars of 1.8 μm thickness with nanostructure and planar Cu electrodes morphology, respectively),[32] Si-based Li-ion battery (90 μA h cm^{-2} at 12 μA cm^{-2} for 0.5 μm of layer thickness),[33] and even when comparing with a 3D configuration (11, 4, and 3.5 μA h cm^{-2} at C/5, 10C, and 20C rates respectively),[39] suggesting that the novel architectured electrode presented here can be a potential candidate for the fabrication of nanostructured thin film microbatteries. Considering Faraday's law, 0.22 mg of tin were electodeposited onto one square centimeter of titania nanotubes; the results expressed in terms of gravimetric capacities are of 675 mA h g^{-1} for first reversible capacity at 2C rate.

To reveal differences in electrode reactions, derivative curves of the cells are shown in Figure 3b,d. The sharpness

(39) Cheah, S. K.; Perre, E.; Rooth, M.; Fondell, M.; Hårsta, A.; Nyholm, L.; Boman, M.; Gustafsson, T.; Lu, J.; Simon, P.; Edström, K. *Nano Lett.* **2009**, *9*, 3230.

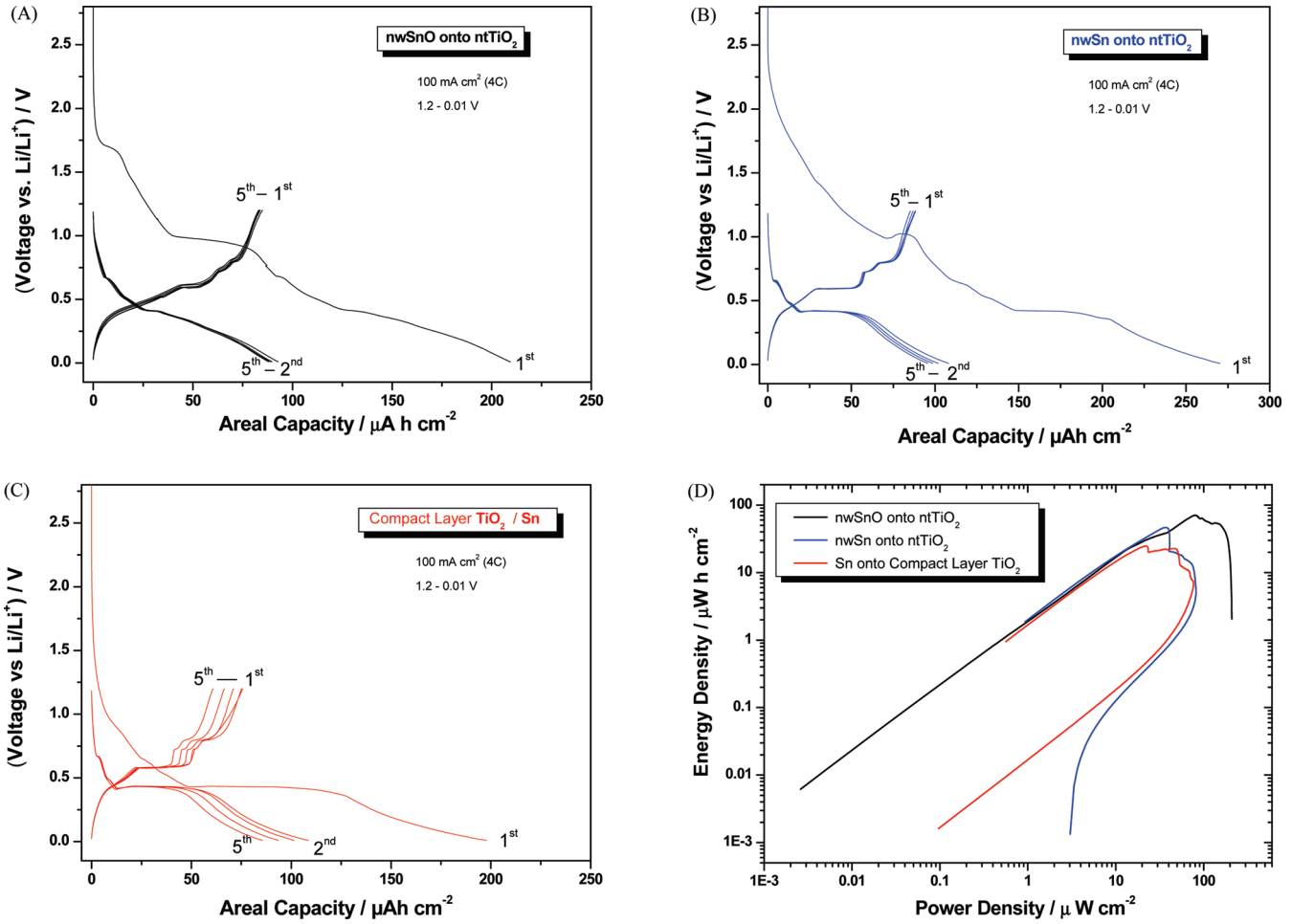

Figure 4. Galvanostaic discharge/charge curves during the first five cycles of (a) crystalline nwSnO/ntTiO$_2$, (c) amorphous nwSn/ntTiO$_2$, and (d) compact layer TiO$_2$/Sn electrodes at 100 μA cm^{-2}. (d) Ragone plots for the three thin film electrodes. Note that the plots are generally based on logarithmic scales.

of the 50th cycle curve has an uncanny resemblance to the first one except for the cut off voltage in charge at 1.2 V. The bottom part indicates the lithiation process, and the upper part shows the delithiation process. Crystalline ntTiO$_2$ reacts with lithium at 1.7 V (Figure 3b); however, amorphous ntTiO$_2$ does not show any contribution (Figure 3c,d). The amorphous state of this non-annealed sample average this contribution to a broadened bands spread between 2.6 and 1.0 V.[28,29] Titania is not further reacting anymore, because of the imposed voltage limitations. The species that are contributing to global reaction in discharge and charge are (i) tin oxide for crystalline samples (1.0 and 0.6 V) and (ii) tin metal for the three samples (0.6 and 0.01 V).

$$\mathrm{ntTiO_2} + x\mathrm{Li^+} + x\mathrm{e^-} \rightarrow \mathrm{ntLi}_x\mathrm{TiO_2} \quad (0 < x < 1)$$

$$\mathrm{SnO} + 2\mathrm{Li^+} + 2\mathrm{e^-} \leftrightarrow \mathrm{Li_2O} + \mathrm{Sn}$$

$$\mathrm{Sn} + x\mathrm{Li^+} + x\mathrm{e^-} \leftrightarrow \mathrm{Li}_x\mathrm{Sn} \quad (0 < x < 4.4)$$

For crystalline electrodes, the loss of initial capacity due to electrolyte decomposition is inevitable and was about 40% of its reversible capacity, since the consumed lithium atoms are irreversibly trapped in first discharge. However, the electrochemical properties of nwSnO in terms of capacity retention/efficiency are very attractive knowing that volume variation of tin-based electrodes range between 200 and 300% during cycling. Bulk tin electrodes tend to pulverize during cycling, and much of the material loses contact with the current collector, resulting in poor transport of electrons. Here nwSn and nwSnO grown directly onto ntTiO$_2$ onto the current collector is probably not pulverized or broken into smaller particles after cycling. Improved strain relaxation allows using nanowires with increased diameter and length without breaking. The nanowire anode configuration can be capable of efficient 1D electron transport. The schematic representation of morphological changes that occur in tin-based electrodes during electrochemical cycling is shown in Figure 3e, indicating such effects by the arrows.

Finally, to better characterize the electrochemical behavior in Li cells of tin-based electrodes onto titania nanotubes, galvanostatic discharge/charge curves are shown in Figure 4a−c, and their capacity values are in consonance with the reversible capacities showed in Figure 3a. Moreover, power vs energy density curves are shown in the Ragone plots in Figure 4d. They are computed here from the 10th discharge curve at a rate of

100 μA cm^{-2}. We have concluded that the electrode of nwSnO/ntTiO$_2$ is capable of providing 75 μW h cm^{-2} of energy density and 85 μW cm^{-2} peak power. Meanwhile, the Sn onto C.L.-TiO$_2$ and nwSn/ntTiO$_2$ electrodes offers 40 and 25 μW cm^{-2} peak power, respectively. One can note that the nanostructured electrodes provide high power and low energy density, in agreement with previous results.[28]

Conclusions

We highlight a novel route for fabrication of nanoarchitectured crystalline nwSnO/ntTiO$_2$ electrodes. The procedure shown here allows obtaining titania nanotubes with 1 μm length after 240 min of titanium anodization, followed by tin electrodepostion under controlled conditions. Optional heat treatments lead to partial crystallization of amorphous titania. The titania nanotubes allow formation of tin nanowires, and this morphology combination permits efficient 1D electron transport and facile strain relaxation of the electroactive material cycled between 1.2 and 0.01 V. The 2 μm length tin-based nanowires supported on self-organized ntTiO$_2$ provide areal capacities of 95 and 140 μA h cm^{-2} ($\sim$675 mAh g^{-1}) under high rates of 100 (4C) and 50 (2C) μA cm^{-2} keeping 70 and 85% initial capacity over 50 cycles, respectively. The preparation of tin in such morphology in combination with titania nanotubes is a new approach that will be helpful for making new nanocomposites for other alternative electrodes, such as manganese, cobalt, or iron-based compounds, if the selected electrochemical parameters are optimized.

Acknowledgment. UCO authors acknowledge financial support from MINN (Contract MAT2008-05880) and Junta de Andalucía (FQM-288 group). Authors are indebted to ANR Programme Blanc 2005 (LIBAN project) and European Research Institute ALISTORE.